

Measurement of Thermal Structure inside Flame Front with a Melting Layer for Downward Flame Spread of XPS Foam

Luo S.F., Xie Q.Y.*, Da L.J.

State Key Laboratory of Fire Science, University of Science and Technology of China,
Hefei, 230027, China

*Corresponding author's email: xqy@ustc.edu.cn

ABSTRACT

Thermal structure of flame front during downward flame spread was experimentally measured with the help of the coordinate transformation method for XPS foam with a thickness of 1.6 cm. Temperature and temperature gradient in the condensed phase, the shape of the molten liquid of XPS fuel, and heat flux through the solid, were obtained. The results show that temperature and temperature gradient gradually decrease from the surface to the inner XPS foam. The temperature distribution also illustrates the shape of the interface between melting liquid and solid. It shows that the interface between the solid and the liquid is flatter in the initial stage than that in the later stage, and the slopes of the solid-liquid interface are in the range about 30-50 degrees. The results also show that the melting layer is thinnest near the flame front and it is thicker for the location farther away from the flame front in the burning area. The molten liquid adheres to the back wall with the downward burning of the XPS sample, which increases the area of the burning surface at the top of the melting layer, and consequently, increases the flame height. In addition, the vertical heat conduction from the melting layer to the unburned zone is calculated by the integration of heat flux along the solid-liquid interface, and the result shows that the average heat flux through solid here is about 580 W/m².

KEYWORDS: XPS foam, downward flame spread, melting layer, thermal structure.

NOMENCLATURE

C	The curve of solid-liquid interface	y	y axis of static coordinate system
k_s	heat conduction coefficient (W/(m·K))	y'	y' axis of moving coordinate system
q_s''	heat conduction through solid phase(W/m ²)	y_c	y_c position of thermocouple tip on static coordinate system
T_m	melting temperature (K)	y'_c	y'_c position of thermocouple tip on moving coordinate system
T_0	initial temperature (K)		
t	time (s)		
w	width of the XPS sample (m)		
x	x axis of static coordinate system		
x'	x' axis of moving coordinate system		
x_c	x_c position of thermocouple tip on static coordinate system		
x_f	x_f position of flame front on static coordinate system		

Greek

δ thickness of XPS sample (m)

Subscripts

0 ambient
 c thermocouple
 f fire
 m melting

INTRODUCTION

Extruded polystyrene (XPS) foams have been widely used as thermal insulation layers in the building wall and roof, refrigeration house and duct of air condition. The fire hazard of XPS foams is a big threat for not only the residents in the buildings but also the firefighters. The Beijing TVCC fire in 2009 is considered as one of the terrible fire accidents with the fastest spread velocity, which is induced by the XPS burning [1]. There are shrinkage, melting, dripping and flowing behaviors during the burning and flame spread of XPS foams. As a typical thermoplastic foam, its burning behavior and flame spread controlling mechanism of vertical or horizontal XPS sheet is obviously different with those traditional solid fuels, such as wood, paper and even PMMA [2-5]. As suggested in previous works, the downward burning of XPS foam is not a conceptually surface flame spread but a downward moving pool fire [1, 6].

The heat transfer, mass transfer and chemical reaction mechanisms in the local region of the flame front play a key role in the flame spread modeling of solid materials. Most of previous experimental works for the controlling mechanism of flame spread of various solid materials mainly focused on the heating of the unburnt surface by flame front, as well as the thermal and flow parameters measurement in the adjacent gas region [7-11]. Recently, Rakesh Ranga and Vasudevan Raghavan investigate the structure and spread rate of flames over PMMA slabs and analyzed flame structure and the temperature field in the gas phase with a 3D-scanning device [12]. For the detailed heat and mass transfer inside the solid materials, especially in the local region of flame front, rare experimental data are available because of the inner measuring difficulty for opaque thick solids and moving behavior of the flame front. However, it is not difficult to inserting thermocouples into the porous polymers. They are good sensors for measuring the temperatures in the burning XPS foam sample. On the other hand, more thermocouples in the XPS foam would be certainly helpful to measure more detailed inner temperatures but also make more disturbance to the sample burning behaviors at the same time. In this work, a method was developed to measure the inner temperatures near the flame front with only a few thermocouples. The detailed temperature field in the condensed phase and the heat transfer mechanism were analyzed for the flame front of XPS foam downward burning based on this method.

EXPERIMENT AND RESULTS

Method for inner thermal structure measurement

The main idea for continuous temperature measurement is based on the relative motion principle. The principle of the method is that the downward movement of the flame relative to the thermocouples can be transformed as the upward movement of the thermocouples relative to the flame. Figure 1 gives the sectional side view for the downward flame spread of XPS foam and two coordinate systems, namely, a static one and a moving one. The origin of the static coordinate system is on the top of XPS foam. The other coordinate system is moving together with the flame front with its origin always on the moving flame front position, which is continuously monitored by a camera. Thermocouples are inserted into the XPS foam. As shown in Fig. 1(a), in the static coordinate system (x, y) , the flame front will pass the thermocouple as the downward burning of XPS foam continues. However, in the moving coordinate system (x', y') , the downward burning is transferred as another behavior as shown in Fig. 1(b). That is, the flame is considered as static, the thermocouple scans to the flame region from the preheat zone and monitors the time-dependent temperature. In this case, the measured time-dependent temperatures by a fixed thermocouple are transformed as space-dependent temperatures in the flame front region by coordinate system transformation with the help of the camera. Therefore, the temperature along the flame spreading direction near the flame front can be measured. This is the main idea for the inner temperature

measurement in this work. In this way, a vertical temperature distribution of the flame front region can be measured by one thermocouple. As shown in Fig. 1(a), for a thermocouple in XPS foam, whose location is (x_{c-i}, y_{c-i}) in the static coordinate system, the measured temperatures can be described as

$$T(x_{c-i}, y_{c-i}) = T(t), \tag{1}$$

where T is the measured temperature by the thermocouple, K , and t is a moment during the XPS foam downward burning, s .

At the moment t , as shown in Fig. 1(a), the location of flame front in the static coordinate system can be addressed as $(x_{f(t)}, 0)$, which is the origin of the moving coordinate and can be continuously measured by a camera. Therefore, the temperatures along the locations with $y = y_{c-i}$ in the flame front region can be achieved.

$$T'(x', y'_{c-i}) = T_{x_{c-i}, y_{c-i}}(t), \quad x' = x_{c-i} - x_{f(t)}, \quad y'_{c-i} = y_{c-i}, \tag{2}$$

where T' is the transformed temperature at location (x', y'_{c-i}) in moving coordinate system, K . $T_{x_{c-i}, y_{c-i}}(t)$ is the measured temperature by the thermocouple at location (x_{c-i}, y_{c-i}) at the moment t . $x_{f(t)}$ is the x-coordinate of flame front at the moment t . The constant x_{c-i} and y_{c-i} are the x-coordinate and y-coordinate of the thermocouple in the static coordinate system.

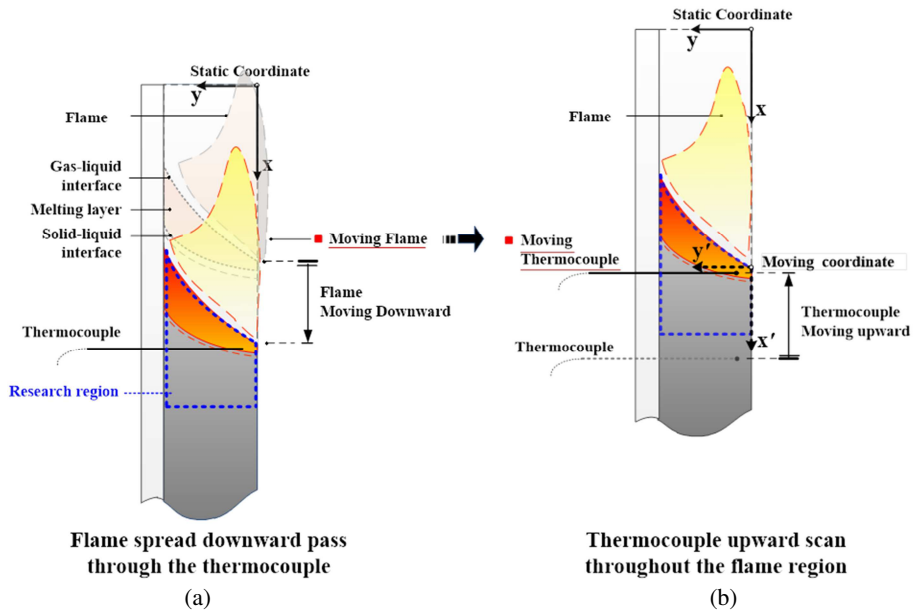


Fig. 1. Schematic of time-space transforming principle in different coordinate system. (a) Downward moving of flame front in a static coordinate system; (b) Upward scanning of thermocouple in moving coordinate system.

Equation (2) shows the method for measuring the vertical temperatures along the flame front through just one thermocouple in the XPS foam by continuously recording the time-dependent temperature. It is suggested that the camera for monitoring the flame front plays a key role in the

“time-space” coordinate transformation. Here several thermocouples at different y -coordinates in the XPS foam are used to measure the temperatures at varied distances to the vertical XPS foam surface. It should be noted that the method developed here is based on the hypothesis of the stable thermal structure of flame spread. As the downward burning of XPS foam is a downward moving pool fire, the temperature distribution in the flame zone varies greatly with time because of the turbulence burning and flame pulsation of the pool fire. Therefore, the temperature there cannot be accurate measured in this way. However, during a short downward flame spread stage, the temperature distribution in the preheated solid and the melting region, as shown in the blue frame in Fig. 1, can be reasonably considered to be stable. Therefore, the temperatures in the XPS foam with condensed phases are the mainly measured here. More details about this method will be shown in the following experimental design and results.

EXPERIMENT

Figure 2 gives the schematic of the experimental setup for the inner temperature measurement during the downward burning of XPS foam. The XPS foam, which is 80cm long and 20cm wide, is vertically adhered to gypsum boards on its back and two sides. The gypsum board is a kind of good thermal insulation material, so the heat loss from the XPS sample to the steel frame is not considered in the heat transfer calculation here.

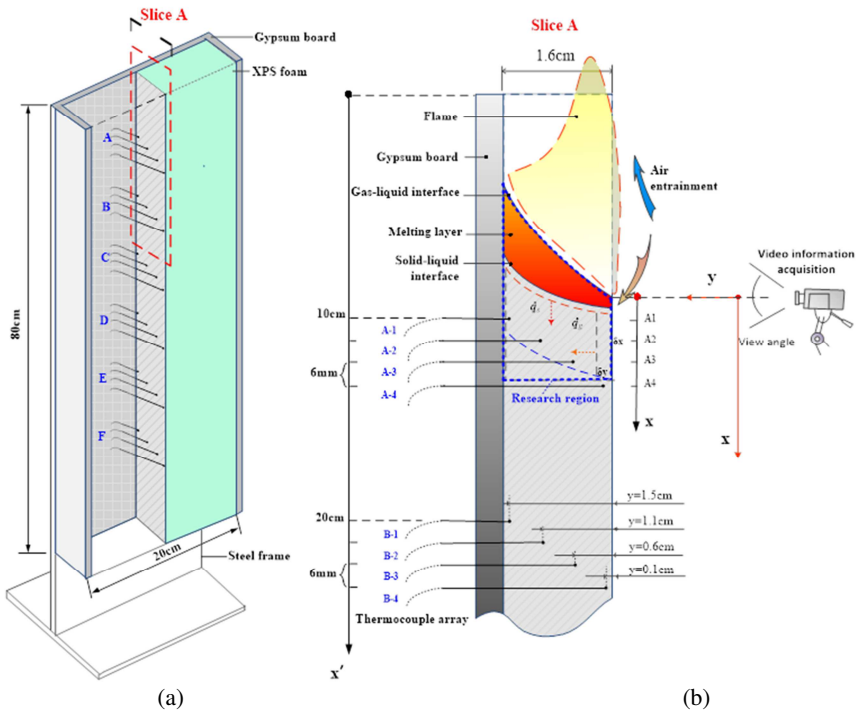


Fig. 2. (a) Schematic of the experimental setup for downward burning of XPS foam with thickness of 1.6 cm; (b) The detailed locations for the six groups of thermocouples.

As shown in Fig. 2(a), 24 thermocouples are located in the central section of the XPS foam. They are divided into six groups for measuring the temperature distribution ahead of the flame front at six stages, respectively. They are Group A, B, C, D, E and F. Fig. 2(b) gives more details about the thermocouples locations in the top two groups, namely, Group A and Group B. As shown in Group

A, four thermocouples were inserted into the XPS foam from the backside with different depths. The distances of the four thermocouple tips with the front surface of XPS foam are respectively 1, 6, 1.1, and 1.5 mm. On the other hand, the vertical distance between the adjacent two thermocouples is 6 mm. The K-type thermocouples with the diameter of 1 mm were used in our research. It is well known that there are less thermal inertia and physical disturbance for thermocouples with a smaller diameter. However, due to the insufficient hardness of the smaller diameter thermocouples, it is not easy to fix the positions of thermocouples when the thermocouples are inserted into the XPS sheets. On the other hand, since the research region of this study is mainly concentrated on the condensed phase with slowly changing temperature, the disturbance of thermocouples to the thermal behavior of fuel is not that much here. According to the tilted shape of the melted layer which will be shown in the section of result and discussion, the inserting depth of the thermocouples at lower positions in Group A is larger. In this way, the interference of the thermocouples on the downward burning of XPS foam is reduced. As shown in Fig. 2(b), the distance between the first thermocouple in Group A and the top of the XPS foam sample is 10 cm. The distance between the two groups of thermocouples is also 10 cm. In this work, experiments were done for XPS foam with thicknesses of 1.6 cm. As shown in Fig. 2(b), the inserting depths of the four thermocouples in each group are 0.1, 0.6, 1.1, and 1.5cm, respectively. Namely, the thermocouples tips are set at 4 positions of $y = 1.5, 0.9, 0.5, 0.1$ cm, where y is the distance from the front surface of the XPS sheet.

As addressed above, a HD camera in front of the XPS foam is used to monitor the downward burning behavior, especially the location of the flame front at the vertical center line. Table 1 gives the physical properties of the XPS foam, which is the typical product commercially available in China. The downward flame spread of XPS foam is ignited with a line of ignition flame on the top.

Table 1. Physical properties of XPS foam

Density of solid foam, kg/m ³	Conductivity, W/(m·K)	Specific heat, J/(kg·K)	Melting temperature, K	Evaporation temperature, K
29.03	0.028	1500	394	503

RESULTS AND DISCUSSIONS

Several runs were carried out for the downward flame spread of XPS foam for repeatability. Here, the main focus will be the temperature processed by coordinate transformation. As discussed in the previous section, the temperature in the flame zone is just the trend of temperature. In this research, the research region is mainly the condensed phase. During a short downward flame spread distance from the beginning preheated solid to the end of the melting region, the temperature in the condensed phase is approximately considered to be relatively stable. As shown in Fig. 2, the 6 thermocouple groups were arranged along the flame spread direction to obtain the temperature distribution at 6 different flame spread stages.

Figure 3 shows a serial of photos of flame near the 6 thermocouple groups in the plane perpendicular to the XPS sample. The thermocouple groups are just under the leading edge of the central flame. The flame leading edge is approximately one-dimensional throughout the experiment, and variation is probably due to surface irregularities and other random factors. It shows that the flame height increase with the downward burning from group A to F, which will be discussed later. Additionally, since the thermocouples were inserted along the vertical symmetrical centerline of the XPS sample, the video camera was used to monitor only the leading edge position of the central flame for the coordinate transformation.

The thermocouples may have some interferences with the heat transfer and the shape of the melting layer. To estimate the disturbances introduced by thermocouples, Fig. 4 gives leading edge position and flame spread rate of the central flame. The positions of the 6 thermocouple groups are also marked on the curve of the leading edge position of the central flame, and the positions of the 6 thermocouple groups are 10, 20, 30, 40, 50, 60 cm, respectively. The flame spread rate over XPS sample is found to be about 0.18cm/s. Although the instantaneous spread rate fluctuates slightly, the averaged spread rate remains relatively steady near the positions with thermocouples or without thermocouples. Therefore, the disturbances introduced by the thermocouples are reasonably not considered in this study.

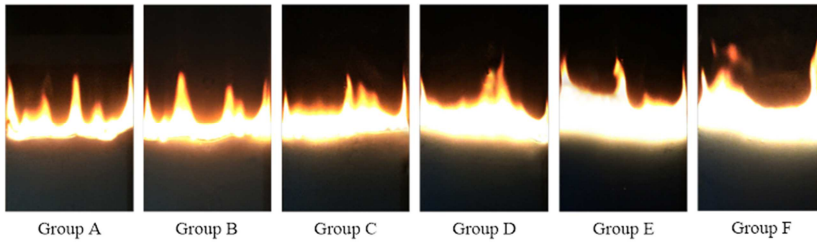


Fig. 3. Photos of flame near the thermocouple groups.

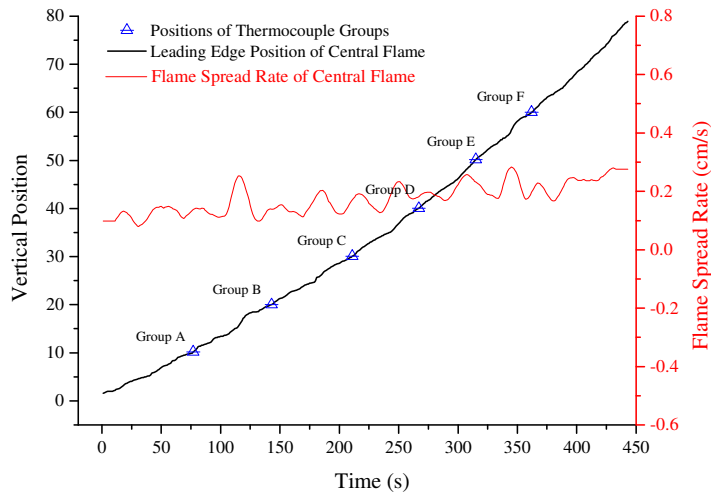


Fig. 4. Downward flame spread Distance and the flame spread rate of the central flame of XPS sample.

Figure 5(a) gives a typical result of the temperature profile measured by the thermocouples of Group D. Note that the x coordinate is not the time, but the difference of vertical position of the thermocouple and the flame front point (see Eq.(2)). The $x = 0$ represents the flame front location based on the video measurement, $x > 0$ defines the preheated zone, and the burning zone is located at $x < 0$. It is seen that the temperature increases quickly when the thermocouple cross the flame zone. The result shows that the temperature of the condensed phase decreases from the surface to the inner solid. Moreover, near $x = 0$, the temperature near the surface starts to rise before the flame front, while the temperature near the backside of solid rises after the flame front. This indicates that the preheat front in the solid phase is tilted outwards. Fig. 5(b) gives the vertical temperature gradient derived by the temperature difference of adjacent nodes in the x -axis direction in Fig. 5(a). It shows that the temperature gradient decrease from the surface to the interior of the XPS fuel, which means that the downward heat transfer in the condensed phase is concentrated in the area close to the solid surface. It can be explained as the effect of the air entrainment of flame and the

difference in oxygen distribution. That is, oxygen in the entrainment air firstly contacts the outer surface of the flame and reacts with the combustible gas generated by the pyrolysis. From the incoming surface to the inner dense material, the oxygen gradually depletes as the oxygen reacts with the pyrolysis gas. Correspondingly, the downward heat transfer through the gas is weakened. Therefore, the temperature gradient at the outer surface of the material is higher than the temperature gradient of the inner side.

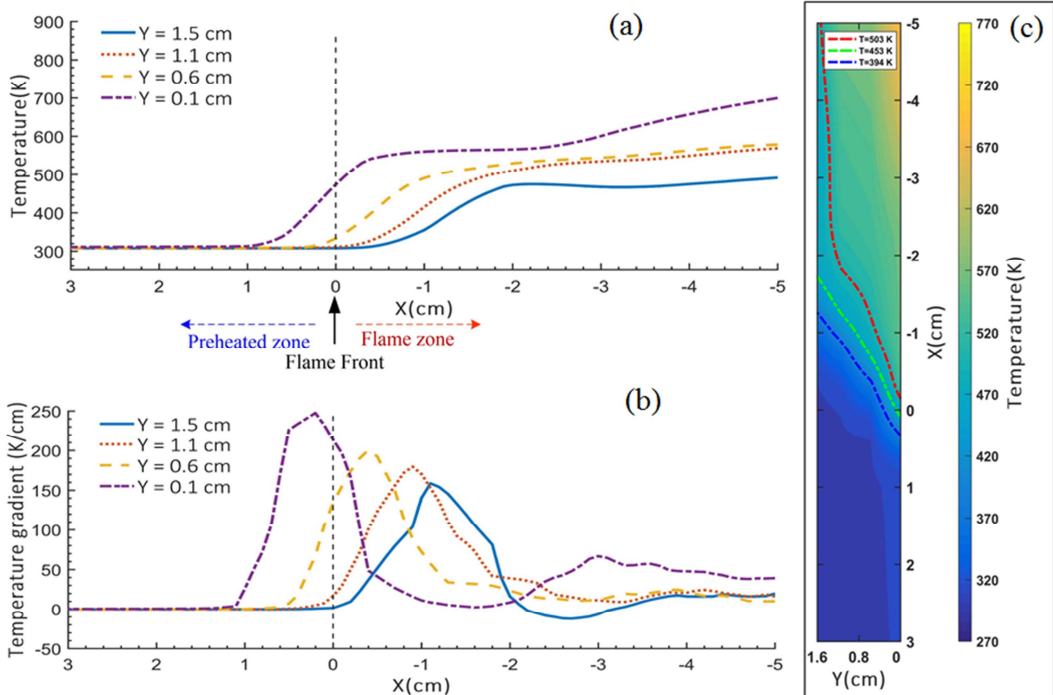


Fig. 5. (a) Temperature profiles in condensed phase at different depth Y; (b) Vertical temperature gradient derived by the temperature difference of adjacent node; (c) Temperature distribution obtained by two-dimensional interpolation.

The temperature distribution of the gas phase and solid for solid PMMA has been analyzed by Ito [13] and Hirano [14] with holographic interferometry. However, It may not easy to obtain the temperature distribution inside XPS solid. Here, the two-dimensional interpolation method is used to construct the inner temperature field of solid. Fig. 5(c) shows the temperature distribution which is obtained by two-dimensional interpolation of the data in Fig. 5(a). It should be noted that the evaporation temperature is about 503 K, above which is the flame region. The temperature above 503 K is not the accurate value because of flame pulsation and the limitation of the thermocouple response time, and it just represents the trend of temperature in the flame area. Three temperature level lines, melting temperature(394 K), evaporation temperature (503 K) and a middle temperature(453 K), are redrawn in the temperature distribution field. According to the vertical distance between the melting temperature line (394 K) and evaporation temperature line (503 K), the melting layer is thinnest near the flame front and it is thicker for the location farther away from the flame front in the burning area.

In addition, there is a clear inclination along the interface between the solid and liquid phases. As discussed in the experimental section, the connection of the four thermocouple tips is an obliquely downward straight line. Therefore, it allows the thermocouple tips to contact the molten interface almost simultaneously. This improves the measurement accuracy of the molten fuel temperature.

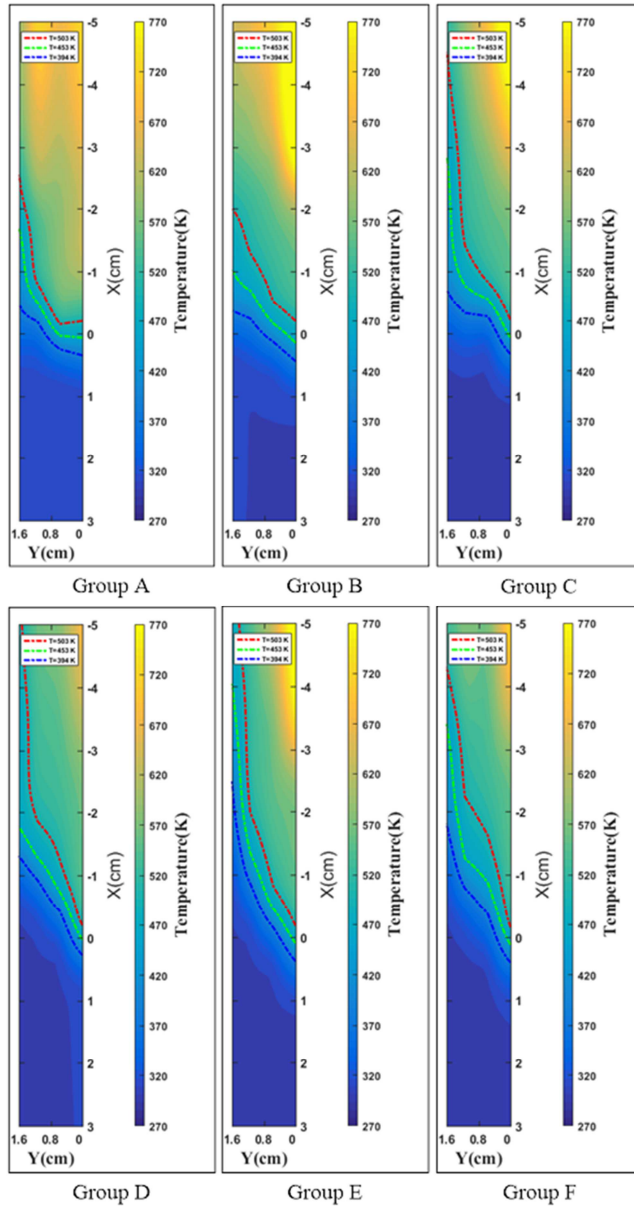


Fig. 6. Contour of temperature distribution at the flame front region on downward flame spread of XPS sample (Group A-F)

Figure 6 gives the all the results of temperature distribution at the flame front region from Group A to F. The results show that the interface between the solid and the liquid is flatter in the initial stage (Group A-C) than that in the later stage(Group D-F), and the slopes of the solid-liquid interface are in the range about 30-50 degrees. The evaporation temperature lines are getting more inclined after Group D, especially the line segment near the back side. This means that molten liquid adheres to the back wall with the downward burning of XPS sample, which increases the area of the burning surface at the top of the melting layer, and consequently, the flame height, as shown in Fig. 3, increases with the downward burning.

Jiang [15] measured the heat conduction through the solid phase by Fourier's law of heat conduction $q''_{s,c} = k_c \partial T / \partial x$, using one thermocouple in solid phase. However, the results of this study show that the temperature and temperature gradient varies greatly from the surface of the sample to the inner solid. Therefore, it cannot be simplified as a one-dimensional heat conduction model. In the case of this research, solid heat conduction into the preheated solid from melting layer through solid $q''_{s,c}$ (W/m^2) can be calculated by the integration of heat flux along the solid-liquid interface

$$q''_s = \int_C w k_s (dT(x, y) / dx)_{T=T_m} dy, \tag{3}$$

where k_s , $\text{W}/(\text{m}\cdot\text{K})$, is the heat conduction coefficient, w (m) is the width of XPS sample, x (m) and y (m) represent the downward and horizontal direction respectively, T_m (K) and C represent the melting temperature and melting interface curve inside the condensed phase, and $(dT(x, y) / dx)_{T=T_m}$ means the vertical temperature gradient along the melting interface.

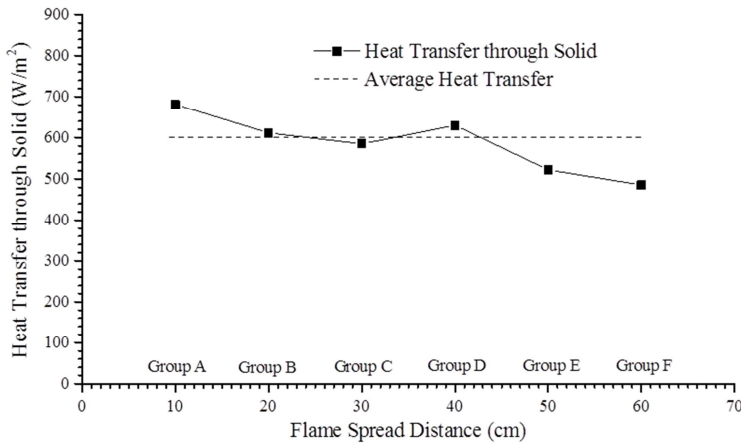


Fig. 7. Heat transfer through solid on downward flame spread of XPS sample.

The temperature profile in Eq. (3) can be obtained from the results of temperature distribution shown in Fig. 6(A-F). Fig. 7 shows the heat fluxes at the solid-liquid interface near the flame front measured by 6 thermocouple groups. As the 6 thermocouple groups are placed at 6 different positions along downward flame spread, the temperature distributions from Group A to F represent the temperature profile at 6 different flame spread distance. In this experimental configuration, the Groups from A to F are corresponding to the flame spread distances from 10 to 60 cm. The result shows that the average heat flux through solid is about $580 \text{ W}/\text{m}^2$.

CONCLUSIONS

In this work, a method is developed to measure the detailed inner thermal structure ahead of the flame front for vertically downward burning XPS sample. The time-dependent temperatures directly measured by the thermocouples in the XPS sample were transformed to the space-dependent temperatures along the flame spread direction based on the method. Following characteristics of thermal structure in the condensed phase have been analyzed. Firstly, the temperature distribution in the condensed phase gives the shape of the molten layer, which shows that the interface between the solid and the liquid is flatter in the initial stage than that in the later stage, and the slopes of the solid-liquid interface are in the range about 30-50 degrees. Secondly, the results also show that the

melting layer is thinnest near the flame front, and it is thicker for the location farther away from the flame front in the burning area. Moreover, the molten liquid adheres to the back wall of the XPS sample with the downward burning, which increases the area of the burning surface at the top of the melting layer, and consequently increases the flame height. In addition, the vertical heat transfer from the condensed phase to the unburned solid zone is calculated by the integration of heat flux along the solid-liquid interface, and the result shows that the average heat flux through the solid is about 580 W/m^2 .

ACKNOWLEDGEMENT

This work was supported by National Natural Science Foundation of China (51476157) and National Key R&D Program of China (2017YFC0805901). The authors appreciate all these supports.

REFERENCES

- [1] S.F. Luo, Q.Y. Xie, X.Y. Tang, R. Qiu and Y. Yang, A quantitative model and the experimental evaluation of the liquid fuel layer for the downward flame spread of XPS foam, *J. Hazard. Mater.* 329 (2017) 30-38.
- [2] A.C. Fernandez-Pello, T. Hirano, Controlling Mechanisms of Flame Spread, *Combust. Sci. Technol.* 32 (2007) 1-31.
- [3] A.C. Fernandez-Pello, Flame Spread Modeling, *Combust. Sci. Technol.* 39 (2007) 119-134.
- [4] A.C. Fernandez-Pello, F.A. Williams, Laminar flame spread over PMMA surfaces, *Proc. Combust. Inst.* 15 (1975) 217-231.
- [5] I.S. Wichman, Theory of opposed-flow flame spread, *Progr. Energy Combust. Sci.* 18 (1992) 553-593.
- [6] W.G. An, H.H. Xiao, J.H. Sun, K.M. Liew, W. Yan, Y. Zhou, Effects of Sample Width and Sidewalls on Downward Flame Spread over XPS Slabs, *Fire Saf. Sci.* 11 (2014) 234-247.
- [7] B. Comas, T. Pujol, Energy Balance Models of Downward Combustion of Parallel Thin Solid Fuels and Comparison to Experiments, *Combust. Sci. Technol.* 85 (2013) 1820-1837.
- [8] S.Y. Hsu, J.S. T'ien, Flame spread over solids in buoyant and forced concurrent flows Model computations and comparison with experiments, *Proc. Combust. Inst.* 33 (2011) 2433-2440.
- [9] W.C. Park, A. Atreya, H.R. Baum, Experimental and theoretical investigation of heat and mass transfer processes during wood pyrolysis, *Combust. Flame.* 157 (2010) 481-494.
- [10] G.L. Juste, L. Contat-Rodrigo, Temperature field reconstruction from phase-map obtained with moiré deflectometry in diffusion flame on solids, *Combust. Sci. Technol.* 179 (2007) 1287-1302.
- [11] S. Bhattacharjee, A. Simsek, F. Miller, S. Olson, P. Ferkul, Radiative, thermal, and kinetic regimes of opposed-flow flame spread A comparison between experiment and theory, *Proc. Combust. Inst.* 36 (2017) 2963-2969.
- [12] H.R. Ranga, O.P. Korobeinichev, A. Harish, V. Raghavan, A. Kumar, I.E. Gerasimov, A.G. Shmakov, Investigation of the structure and spread rate of flames over PMMA slabs. *Appl. Thermal Eng.*, 130 (2018) 477-491.
- [13] A. Ito, T. Kashiwagi, Temperature measurements in PMMA during downward flame spread in air using holographic interferometry, *Proc. Combust. Inst.* 21 (1988) 65-74.
- [14] T. Hirano, K. Sato, Effects of radiation and convection on gas velocity and temperature profiles of flames spreading over paper, *Proc. Combust. Inst.* 15 (1975) 233-241.
- [15] L. Jiang, C.H. Miller, M.J. Gollner, J.H. Sun, Sample width and thickness effects on horizontal flame spread over a thin PMMA surface, *Proc. Combust. Inst.* 36 (2017) 2987-2994.